An automatic algorithm for distinguishing optical navigation markers used during surgery

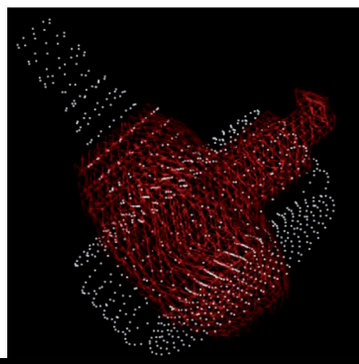

UN ALGORITMO AUTOMÁTICO PARA DISTINGUIR LOS MARCADORES OPTICOS DE NAVEGACIÓN UTILIZADOS DURANTE LA CIRUGÍA

DOI: http://dx.doi.org/10.6036/7494 | Received: 04/dec/2014 • Accepted: 13/jan/2015

Ken Cai[1,3], Rongqian Yang[2], Hai Ning[2], Shanxin Ou[3], and ZhaoFeng Zeng[4]

[1] School of Information Science and Technology, Zhongkai University of Agriculture and Engineering, Zhongkai Road 501#, Guangzhou, 510225, Guangdong, China

[2] Department of Biomedical Engineering, South China University of Technology, HEMC, Guangzhou, 510006, Guangdong, China, kyscut@126.com

[3] Department of Radiology, General Hospital of Guangzhou Military Command of PLA, Liuhua Road 111#, Guangzhou, 510010, Guangdong, China

[4] Department of Mathematics and Computer Science, California State University, East Bay ,25800 Carlos Bee Boulevard Hayward, CA 94542, U.S.A

RESUMEN

• Con el fin de mejorar la seguridad, la exactitud y la eficacia de la cirugía, reduciendo el trauma quirúrgico, la posición espacial tridimensional de los instrumentos quirúrgicos se puede lograr a través de la precisión de la integración de las imágenes médicas para guiar su funcionamiento durante la cirugía. Por lo tanto, antes de la cirugía, el registro es necesario para establecer la relación entre la posición real de los instrumentos quirúrgicos y sus imágenes. La precisión de este tipo de registro determina directamente la precisión de la navegación. Teniendo en cuenta los problemas y las deficiencias de los actuales métodos de registro del marcador de referencia, en este trabajo se propone la extracción de un marcador de referencia automático y algoritmo de coincidencia. Con el fin de facilitar reconocimiento automático y extracción de los marcadores de referencia los autores de este documento diseñaron un marcador de referencia con tomografía axial computarizada (TAC) de valores y formas reconocibles que proporcionan características que ayudan a satisfacer las demandas de los requisitos de posicionamiento. La extracción de estos marcadores de referencia se puede automatizar fácilmente, lo que reduce considerablemente la dificultad de desarrollar un algoritmo extracción. Después de la extracción del marcador de referencia el registro de algoritmo iterativo y el punto más cercano (ICP) algoritmo pueden ser combinadas para lograr coincidencias entre el marcador y punto set model del marcador de referencia. De acuerdo a los resultados coincidentes que indica la relación de posición entre cada marcador y su reflectante, el centro de la esfera reflectante de la imagen puede ser adquirido, proporcionando así una forma sencilla de realizar el registro de las diferentes representaciones espaciales del paciente.

• **Palabras clave:** marcador de referencia, iteración del punto más cercano (IPC), navegación óptica.

ABSTRACT

To improve the safety, accuracy and effectiveness of surgery, while also reducing surgical trauma, three-dimensional spatial positioning of the surgical instruments can be achieved through the accuracy of integration of medical imaging to guide their operation during surgery. Therefore, prior to surgery, registration is required to establish the relationship between the actual positioning of the surgical instruments and their imaged position. The accuracy of such registration directly determines the precision of navigation. Taking into account the shortcomings and deficiencies of the current fiducial marker registration methods, this paper proposes an automatic fiducial marker extraction and matching algorithm. In order to facilitate automatic recognition and extraction of the fiducial markers the authors of this paper designed fiducial marker with Computed Tomography (CT) values and shapes that provide recognizable characteristics which help to meet the demands of the positioning requirements. The extraction of such fiducial markers can be easily automated, significantly reducing the difficulty in developing an extraction algorithm. After fiducial marker extraction the registration algorithm and the Iterative Closest Point (ICP) algorithm can be combined to achieve matching between the fiducial marker and point set model of the fiducial marker. According to the matching results indicating the positional relationship between the each fiducial marker and its retroreflective sphere, the center coordinate of the retroreflective sphere in the image can be acquired, hence providing an easy way to undertake registration of the different spatial representations of the patient.

Keywords: Fiducial marker, ICP, Optical navigation.

INTRODUCTION

With the in-depth application of computer technology in the medical field and the emphasis on the surgical refinement and minimal invasion, the surgical navigation system has become a new hotspot for research and clinical application in the field of medical equipments. Cancer treatment by radiofrequency ablation guided by images has been widely applied, including treating the tumors in liver[1-3], kidney[4], bone[5,6], breast[7,8] and lung[9,10]. The surgical navigation system usually consists of visual parts and measuring equipments which can position and track the relative position between surgical instruments and patients. Nowadays, the mainstream measuring equipment used in the surgical

navigation is the optical positioning and tracking system.Prior to using the optical tracking system to start the tracking and positioning of surgical instruments, the mapping relationship between the operation space and the image space, namely registration, must be established. Ahead of this, the center coordinates of the fiducial markers used for registration of the image of the patient, in the image space and in the operation space must both be determined. On the basis of these two sets of coordinates, the positional relationship between the image space and the operation space can be acquired as a matrix of a series of rotations and translations in order to complete the registration. The current, commonly used approaches to registration are either surface-based or fiducial marker-based methods [11]. The former does not require fiducial markers. It matches the surface information for the actual space, obtained using an optical method, to a surface representation extracted from the image space [12, 13]. This method is rarely used due to the inaccuracy of registration resulting from its complicated system design and simple operation[14]. By contrast, the second method, has greater accuracy, and is the more commonly used nowadays [15]. However, manual difference of human positioning and such positioning of the fiducial marker will also add a registration error [16-18]. This because the fiducial marker registration often requires a manual approach to extract the center coordinates, both the pixel pitch and the layer thickness of the image, as well as, mean that such an approach using the center coordinates for registration may result in individual deviations. This deviation will, then, always be present as a system error during both tracking and positioning, severely affecting the tracking precision. Therefore, it is critical to be able to extract and match the fiducial markers within the image automatically. This paper proposes an algorithm for the automatic extraction and matching of fiducial markers. This algorithm, used with a bespoke design of fiducial markers, can quickly and conveniently extract fiducial markers from the image; match all the fiducial markers with the affine transformation and optimize the registration results using the Iterative Closest Point (ICP) algorithm. According to the matching results and the fixed positional relationship between each fiducial marker and its retroreflective sphere, the center coordinates of the retroreflective sphere in the image space can be acquired. In the operation space, the binocular vision system can identify the retroreflective sphere by its regular shape, hence its center coordinates can be obtained. Once the image of the retroreflective sphere and its center coordinates in the operation space have been matched, the patient registration is complete.

2. METHOD

2.1. DESIGN OF FIDUCIAL MARKERS

A retroreflective sphere reflecting near-infrared light can be clearly identified by using the optical positioning facility of the optical surgical navigation system. However, in the image of the patient, the brightness of the retroreflective sphere is relatively low, as it is close to the CT value of most human tissues, so it is difficult to extract the retroreflective sphere automatically so as to acquire its coordinates. Therefore, high-brightness fiducial markers with high-CT values are needed allowing for easy extraction when interfacing with the retroreflective sphere. The materials commonly used for fiducial markers are stainless steel or plastic, however stainless steel fiducial markers produce artifacts, which can reduce the quality of the image and influence the doctor's surgery. Furthermore the brightness in the image of such commonly-used fiducial marker materials is low, as the differences between their gray levels and those of human tissues are not significant, so they are not easy to identify and it is therefore difficult to develop an automatic extraction algorithm for such fiducial markers. In order to reduce this difficulty in extracting the fiducial markers from the image as reference points when using the retroreflective sphere model [19], the solution is to design fiducial markers with high CT values, as shown in Fig.1(a) and Fig.1(b). Fig.1(c) and Fig.1(d) which are based on the physical shape of the fiducial marker so as to simulate the model of the same shape on the computer and form the point sets. When conducting registration, the fiducial markers should be attached to the patient's skin for positioning purposes. To prevent any slippage, the base of the fiducial marker needs sufficient size to allow for its secure attachment to the skin by using an adhesive. In the process of positioning, the fiducial marker it should be interfaced with the retroreflective sphere, the surface of which is covered with special reflective materials; the fiducial marker must be embedded into the retroreflective sphere. Therefore, the authors of this paper marked the groove shaped retroreflective sphere as a reference object to design the protrusion. The fiducial marker can be interfaced with a retroreflective sphere, to complete the positioning in the operation space.

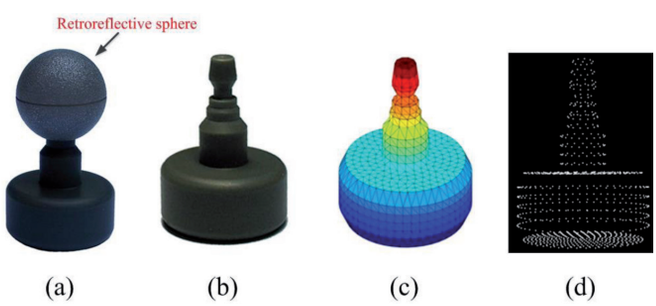

Fig. 1: The bespoke fiducial marker. (a) The retroreflective sphere and the fiducial marker.(b) The actual fiducial marker.(c) Grid model of the fiducial marker.(d) Point set model of the fiducial marker

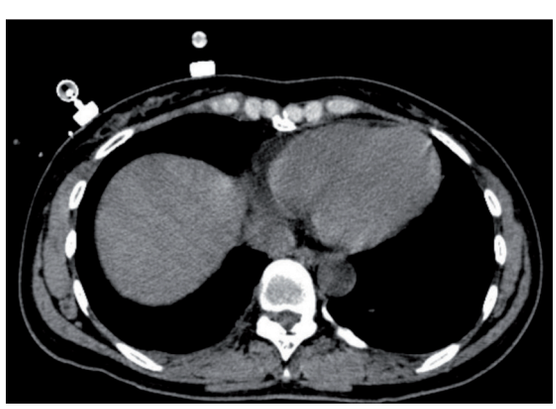

Fig. 2: The CT image

Due to the special material used and its higher CT value, its gray level is significantly higher than that of the retroreflective sphere and of most of the human tissues in the image of the patient, as shown in Fig.2.

In order to extract the fiducial marker, firstly, the Marching Cube (MC) algorithm is used to formulate a surface rendering on the patient's celiac image [20]:

$$\{(x,y,z)\,|\,f(x,y,z)=\boldsymbol{C}\} \tag{1}$$

where (x,y,z) is a space coordinate of a point in the iso surface, $f(x,y,z)$ is a iso surface function, $\boldsymbol{C}$ is a iso surface threshold. The basic procedures of Marching Cubes Algorithm are: first, the two-dimensional slice images are read-in out of three-dimensional data base, and the adjacent two pieces of two-dimensional slices combines as one layer; Second, in each layer, the two two-dimensional slices correspond to 2×2 pixel forming a cube which has 8 vertex; third, each such cube is processed as per threshold value $\boldsymbol{C}$ in the sequence from left side to right, front side to back, and bottom to up; last, draw triangular patch collection which has been processed above as per illumination model. A lot of noise will occur during surface rendering , and there are many tiny tissues in this region, which will affect the extraction of the fiducial marker, so median filtering is needed for rendering of the surface in this case [21]:

$$\hat{Y}_{ij}=\text{median}\{X_{ij},X_{lm},(l,m)\in\Psi_{ij}\setminus M,X_{lm},(l,m)\in\Psi_{ij}\setminus M,Y_{lm},(l,m)\in\Psi_{ij}\cap M\} \tag{2}$$

where X_{ij} is any noise pixel, M is the noise candidate set, Ψ_{ij} is the set of the four closest neighbors of (i,j). Secondly, threshold segmentation is carried out on the filtering results. Threshold processing can not only filter out the retroreflective sphere and other interference having smaller CT values, but can also distinguish the fiducial markers from the human tissues. By this method, only the fiducial markers, bones, Radio Frequency (RF) electrode and other components are identified with high gray levels, allowing the fiducial markers and the skin tissue to be distinguished. A binary image is obtained through binarization of the threshold processing results. In this case, there are only tissues with higher gray levels, namely the bones and the fiducial markers, in the image. A connected component labeling algorithm can be used to mark the binary image[22]. Firstly, the image is scanned from left to right and top to bottom. The current pixel q is computed by:

$$s(x,y)=\begin{cases}Q_B, b(x,y)=Q_B\\ m,(m=m+1),\forall(i,j)\in U_s, s(x-i,y-j)=Q_B\\ L_{min}(x,y),\text{other}\end{cases} \tag{3}$$

where b(x,y) is a pixel value of binary image, Q_B is the background pixels, U_s is a pixel set of template neighborhood excluding current pixel q, the $L_{min}(x,y)$ is given by:

$$L_{min}(x,y)=\min\{L[s(x-i,y-j)]\,|\,i,j\in U_s\} \tag{4}$$

where L is a one-dimensional array for recording the equivalence relationships of connected component labeling. At the same time, the L is assigned by:

$$\begin{cases}\text{nop}, b(x,y)=Q_B\\ L[m]=m,\forall(i,j)\in U_s, s(x-i,y-j)=Q_B\\ L[s(x-i,y-j)]=L_{min}(x,y), s(x-i,y-j)\neq Q_B\end{cases} \tag{5}$$

Secondly, the forward and backward scanning is implemented sequentially after the first scanning is completed.

$$s(x,y)=\begin{cases}Q_B, b(x,y)=Q_B\\ L^U_{min}(x,y),\text{other}\end{cases} \tag{6}$$

where $L^U_{min}(x,y)$ can be expressed as:

$$L^U_{min}(x,y)=\min\{L[s(x-i,y-j)]\,|\,i,j\in U\} \tag{7}$$

where U is a pixel set of template neighborhood. Meanwhile, the L is assigned by:

$$\begin{cases}\text{nop}, b(x,y)=Q_B\\ L[s(x-i,y-j)]=L^U_{min}(x,y), s(x-i,y-j)\neq Q_B\end{cases} \tag{8}$$

Finally, the scanning does not stop until the pixel label is no longer changed:

$$L[s(x-i,y-j)]=L_{min}(x,y)\ \text{ if }\ s(x-i,y-j)\neq Q_B\ \text{ where }\ (i,j)\in U_s \tag{9}$$

According to the actual volume of the fiducial marker and the interval of voxels in the 3 Dimensions (3D) image, we can calculate the number of voxels of the fiducial marker in the image, and set the marked range of voxels. Meanwhile we can calculate the number of voxels contained in each connected component, and extract the connected component from within the selection range. This method can extract all the fiducial markers, unfortunately tissues where the voxel content is similar to that of the fiducial markers (such as ribs) will also be extracted. Anyway, the special shape of the fiducial marker and its unique structural differences from human tissue enable it to be distinguished because of its shape and size. Depending on the actual size of the fiducial marker, we can set the maximum spacing of any two voxels in the connected components, and calculate the maximum spacing of the two voxels in each connected component in the 3D image obtained after the initial filtering. At the same time, this retains the maximum separation over the greatest range of spacing of the connected components, and effectively filters the non-fiducial marker components. As a result, we obtain a three-dimensional image showing only the fiducial markers. It is worth noting that, as a result of the multi-step image pre-processing, even where the actual shapes of the human tissues and the fiducial markers is significantly different, after filtering and smoothing, their representations may appear similar in shape. Therefore, in order to counter this potential defect in the algorithm in dealing with these special circumstances, we can optimize by filtering from the matching error of the extractive results and the fiducial marker models. Specifically, each initial extractive connected component is matched against the fiducial marker model and any one which shows a relatively large registration error is thus identified as being an unmarked tissue, while any other displaying only a minimal error is identified as a fiducial

marker. Using this principle, extracting only those connected components showing minimal errors, can identify the fiducial markers. According to the accuracy of the registration, eliminating any tissue with significant registration errors allows for accurate extraction this as well.

2.2. THE AUTOMATIC EXTRACTION AND MATCHING ALGORITHM

As shown in Fig. 3, $\boldsymbol{P}_m$, the point set of the fiducial marker model, is far away from $\boldsymbol{P}_f$, the point set of the extractive results of the fiducial markers in the visualization representation. When the fiducial marker registration is made through directly using the traditional point set matching algorithm, more extensive calculation is required and the matching efficiency is lower, thus also reducing the success of registration.

Fig. 3: The extractive results of the fiducial marker and of the point set of the model before registration

ICP algorithm has a certain defect for it has to set an initial iteration value which it is prior to continue the sequent registration; if initial iteration value is inapproriate, the algorithm will reduce and be limited to local optimization hence the iteration fails to acquire the accurate registration. Therefore, in order to improve the operational efficiency and overcome the defects of the registration algorithm, this paper proposes the use of an automatic extraction and matching algorithm for the fiducial markers. Firstly, using the center coordinates of $\boldsymbol{P}_m$ and $\boldsymbol{P}_f$, we move $\boldsymbol{P}_m$ to make it to coincide with the center of $\boldsymbol{P}_f$. Then, by rotating $\boldsymbol{P}_m$, we can optimize the registration results in terms of the angle, and complete the initial registration of the fiducial marker.

$$\begin{bmatrix} x_f \\ y_f \\ z_f \end{bmatrix} = \boldsymbol{R}^0 \begin{bmatrix} x_m \\ y_m \\ z_m \end{bmatrix} + \boldsymbol{t}_c \tag{10}$$

where (x_f,y_f,z_f) is the center coordinates of $\boldsymbol{P}_m$, (x_m,y_m,z_m) is the center coordinates of $\boldsymbol{P}_f$, $\boldsymbol{R}^0$ is the rotation matrix, $\boldsymbol{t}_c$ is the translation vector.

The final registration results can then be obtained by adopting the ICP algorithm. In this way, this approach can effectively overcome the ICP algorithm defect of too easily obtaining an inappropriate local minimum value. The ICP algorithm, which is at the core of the majority of point cloud registration algorithms, is a point-to-point rigid registration algorithm. The basic idea is as follows: suppose the two point sets $\boldsymbol{P}$ and $\boldsymbol{Q}_0$ are approximate aligned and the closest point of $\boldsymbol{Q}_0$ is aligned with each point of $\boldsymbol{P}$. Next, use a closest point search respectively to identify each corresponding closest point of $\boldsymbol{P}$ on $\boldsymbol{Q}_0$, which consequently will form set $\boldsymbol{Q}$. Furthermore, by adopting the least squares method to calculate the optimal rigid transformation from $\boldsymbol{P}$ to $\boldsymbol{Q}$, namely the rotation matrix $\boldsymbol{R}$ and the translation matrix $\boldsymbol{T}$, this makes the error function minimal:

$$E(\boldsymbol{R},\boldsymbol{T}) = \frac{1}{n}\sum_{k=1}^{n}\left\| q_k - (\boldsymbol{R}\times p_k + \boldsymbol{T})\right\| \tag{11}$$

The new point collection $\boldsymbol{Q}_1$ acquired after the registration conducts rigid transformation with $\boldsymbol{P}$ using iteration. Iteration does not stop until the registration error E reaches the minimum value or less than the previous set value.

3. EXPERIMENTS

3.1. THE AUTOMATIC EXTRACTION EXPERIMENT

Since the luminous balls cannot be directly used for matching, this paper designs a kind of fiducial markers with a higher CT value for matching. Such mark points can be embedded into the groove of luminous balls and applied in the optical positioning system. Through filter processing, threshold segmentation, connected component labeling and other algorithms, the marked points are extracted from the complex image background, and the model data of mark points and the extracted results are registered. By use of the positional relation between mark points and luminous balls, the center coordinates of luminous balls are obtained, namely the image space coordinates. The specific operation process of automatic extraction algorithm of mark points is as follows:

(1) For abdomen CT images, use the MC algorithm to conduct the surface rendering so as to obtain the image $\boldsymbol{I}_O$;
(2) For the surface rendering image $\boldsymbol{I}_O$, conduct the filtering threshold processing so as to obtain the processing results $\boldsymbol{I}_T$;
(3) Conduct binaryzation for $\boldsymbol{I}_T$, so as to obtain the binary image $\boldsymbol{I}_B$;
(4) Make 3D mark image $\boldsymbol{I}_L$, and all the voxel values are initialized to 0; Establish a new linked list ***ConLt***, and save the information of the connected region;
(5) Traverse $\boldsymbol{I}_B$ from the first voxel;
(6) Dispose 1 in the corresponding position of $\boldsymbol{I}_L$ until encountering the voxel $\boldsymbol{P}_l$ unequal to 0.
(7) Conduct 26 neighborhood search from $\boldsymbol{P}_l$, and find the voxel connected to $\boldsymbol{P}_l$ and with a gray value unequal to 0; Write down the eligible voxel number and add into ***ConLt***;
(8) Dispose all the neighborhood points of $\boldsymbol{P}_l$ in the same way, and the final research result is that the connected region where $\boldsymbol{P}_l$ is located is marked as 1, and the 0^{th} node of ***ConLt*** saves the voxel number marked as 1;
(9) Repeat 5-7, and if the traversed voxel has been marked at the corresponding position of $\boldsymbol{I}_L$ (that is, the voxel value of $\boldsymbol{I}_L$ at this position is not 0), then this point should be ignored; Otherwise, it should be marked, and the marking value is the size of ***ConLt*** + 1.

The Marching Cube algorithm was used to reconstruct a three-dimensional image of the patient's abdomen, with the iso surface threshold set to 80 HU. The rendering results are as shown in Fig. 4. From this it can be clearly seen that there are four fiducial markers attached to the patient's skin.

Fig. 4: The surface rendering image

In order to reduce noise and the interference from other small tissues in the image, median filtering was conducted for the surface rendering results. In this case the gray level of each pixel in the volume data field was set to the median value of the gray level of all the neighborhood pixels. The filtering results are as shown in Fig. 5. Most of the noise has been filtered out, but the fiducial markers are unaffected.

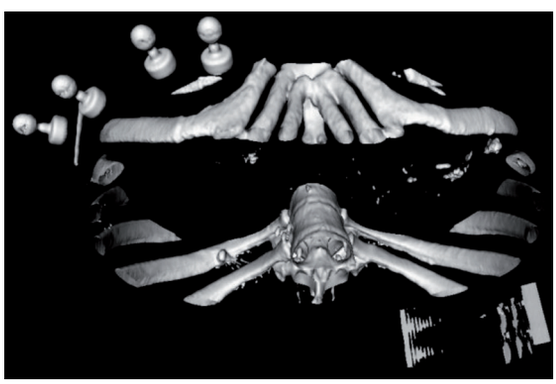

Fig. 5: The median filtering image

For the purposes of this paper the threshold value for threshold processing was set to 500 HU. As the CT value of the retroreflective sphere is relatively low, this means that the influence of the filtering algorithm on it is relatively large, so it is difficult to adopt the general algorithm to extract it completely. As a result, the space coordinate of the image of the retroreflective sphere is obtained indirectly through its registration fiducial markers. Threshold processing can remove the retroreflective sphere and other interference having smaller CT values, while it can still discriminate the fiducial markers from the human tissues, as shown in Fig. 6.

Fig. 6: The threshold processing image

A connected component labeling algorithm was adopted to mark the binary image. The labeling results consist of 108 connected components, among which, the largest connected component contains 7151 voxels, while the smallest contains only a single voxel. The results are presented in Fig. 7.

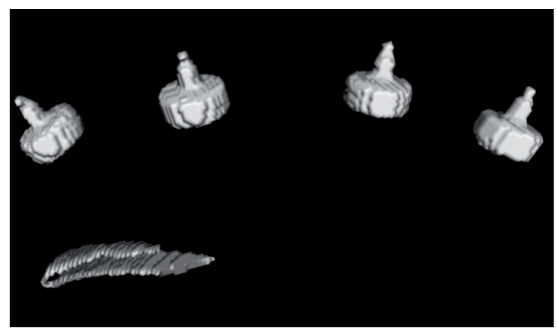

Fig. 7: The connected component labeling image

The tissues extracted by the above method only contain a small number of interference components together with the fiducial markers. The number of voxels in the interference components is similar to that in the fiducial markers. However, because of the unique shape of the fiducial markers and the significant structural differences between these and the human tissues, the fiducial markers can be extracted through distinguishing their shape and size as shown in Fig. 8.

Fig. 8: The accurate extraction image

3.2. THE REGISTRATION EXPERIMENT

In this paper, $\boldsymbol{P}_m$, the point set of the fiducial marker model, contains 969 points, and the center coordinate of the point set can be represented as $\boldsymbol{C}_m$ = {-3.86xe^{-16}, 2.70xe^{-17},4.50}. The point set of $\boldsymbol{P}_f$ contains 3119 points, and the center coordinate of the point set can be expressed as $\boldsymbol{C}_f$= {-19.60, 54.07,34.44}. Thus, according to the center point registration, we can obtain a translation matrix for the two groups of point sets, which can be given as $\boldsymbol{t}_c$ = {-19.60, 54.07, 29.94}. If we move $\boldsymbol{P}_m$ to coincide with $\boldsymbol{t}_c$, the results of this move are as shown in Fig. 9. Obviously, while the registration results make the center of the model consistent with the center of the extractive results, there is a large deviation in angles.

On the basis of the center point registration, we then make an affine transformation on the registration results, and through automatically rotating the model, can find the rotation angle when the registration error is minimal. In this way, the

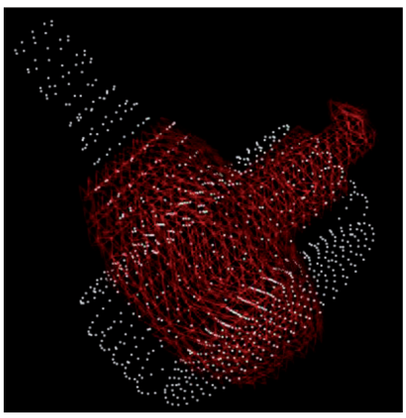

Fig. 9: The center registration image of the fiducial marker

registration effect can be further optimized. This paper selects the point set of the rotation fiducial marker model with its rotation center being the center of the set point of the model. The interval of the rotation angle is A_R, and the rotation results are as shown in Fig. 10. Compared with the registration results based on moving the center point, they have greatly optimized the angle. The interval of the setting rotation angle is 45°, so the registration results after rotation will lead to error.

Experiment shows that the smaller the angle interval A_R, the smaller the registration error will be. However, if A_R is too small, the fiducial marker's rotation times will be increased. Correspondingly, the extent of required calculation will also

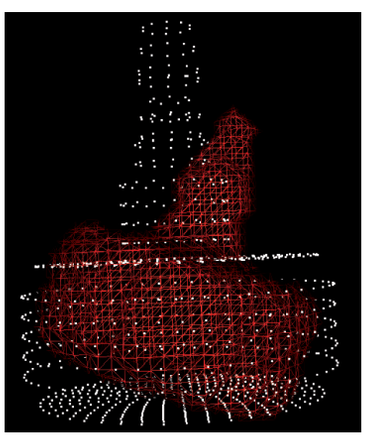

Fig. 10: The registration image of the fiducial marker after rotation

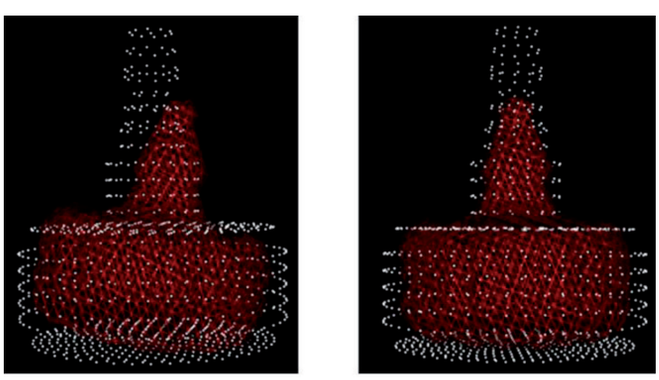

(a) (b)

Fig. 11: Comparison of the fiducial marker rotation results according to different angles. (a) The rotation results with an angle of 30°. (b) The rotation results with an angle of 10°

increase, and the overall registration process will take longer. Therefore, in practice, there is a need to balance reasonable registration accuracy against the time required for determining it. In Fig.11(a), when A_R is 30°, the minimum registration error is 1.161 mm and the rotation is 72 times. It can be seen from Fig.11(b) that when A_R is 10°, the minimum registration error is 1.08 mm and the rotation is 648 times.

Based on the initial matching of the fiducial marker, the ICP algorithm can be used to optimize the registration results, and the final optimization results are as shown in Fig.12. It can be seen that the registration effect of the fiducial marker model and the extractive results are good and the registration error is 1.018 mm.

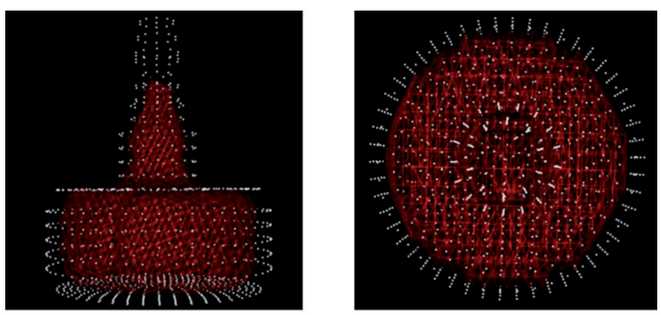

(a) (b)

Fig. 12: The ICP optimization results of the fiducial markers. (a) Side view of registration results.(b) Vertical view of registration results

4. DISCUSSION AND CONCLUSION

The optical surgical navigation system is applied in the treatment of radiofrequency ablation. Before the surgery, the patient's image is input into the image processing and control system, and 3D reconstruction is done to the patient's image, after which the surgery is simulated by use of the optical surgical navigation system so as to specify the optimal surgical plan. Then, the luminous balls tagged on the patient are identified by using the optical positioning system so as to obtain the space coordinates of the luminous balls. Then, the space coordinates of the luminous balls in the image are indirectly obtained through the mark points, and the surgical coordinates and the image space coordinates of the luminous balls are matched, so as to obtain the mapping relationship of the image space and the surgical space. Therefore, to achieve this, this paper proposes the use of a fiducial marker design with both a high-CT value and a unique shape which is consistent with the positioning requirements. Moreover, through computation methods such as filtering, threshold segmentation and connected component labeling algorithms, the fiducial markers can be discriminated from complex image background, laying down the foundations for applying the subsequent registration algorithm to the fiducial markers. As the ICP algorithm is prone to cause inapporiate local minimum value, the paper proposes the use of an automatic registration algorithm for identifying the fiducial markers. Firstly, in accordance with the centers of the model point set and the data point set, we calculate the translation matrix of the two centers; then use the translation matrix to move the model point set in order to make the two centers overlap. Where the two groups of point sets intersect and initially register by using the acquired fiducial markers; hence the less calculation of subsequent registration will be conducted, and the registration rate will be optimized. In addition, affine

transformation can be used to optimize the registration results in terms of the angle; lastly, the final registration results are obtained by adopting the ICP algorithm. Using this approach can effectively overcome the defect of inapporiate local minimum value by using ICP algorithm. The experimental results show that the registration method can provide for effective registration of the fiducial marker model and the extractive results.

APPRECIATION

This research was funded by the China Postdoctoral Science Foundation under Grant No.2013M542158, the Guangdong Natural Science Foundation under Grant No.S2013040014993, the State Scholarship Fund under Grant CSC NO.201408440326, the Social Development and Technology Projects in Guangdong Province under Grant No.20120318057, the Pearl River Nova Program of Guangzhou under Grant No.2014J2200049, the National Natural Science Foundation of China under Grant No.81101130, the Guangdong Provincial Science and Technology Program under Grant No. 2012B031800026, and the Fundamental Research Funds for the Central Universities under Grant No.2014ZG003D. This research was performed in cooperation with the HuaBo Bio-Pharmaceutic Institute of GuangZhou.

BIBLIOGRAPHY

[1] Livraghi T, Goldberg SN, Lazzaroni S, et al. "Hepatocellular carcinoma: radio-frequency ablation of medium and large lesions". Radiology. March 2000. Vol. 214-3. p.761-768. DOI: http://dx.doi.org/10.1148/radiology.214.3.r00mr02761

[2] Lencioni R, Cioni D, Bartolozzi C. "Percutaneous radiofrequency thermal ablation of liver malignancies: techniques, indications, imaging findings, and clinical results". Abdom Imaging. August 2001. Vol. 26-4. p.345-360. DOI: http://dx.doi.org/10.1007/s002610000194

[3] Solbiati L, Livraghi T, Goldberg SN, et al. "Percutaneous radio-frequency ablation of hepatic metastases from colorectal cancer: long-term results in 117 patients". Radiology. October 2001. Vol. 221-1. p.159-166. DOI: http://dx.doi.org/10.1148/radiol.2211001624

[4] Hines-Peralta A, Goldberg SN. "Review of radiofrequency ablation for renal cell carcinoma". Clinical Cancer Research. September 2004. Vol. 10-18. p.6328S-6334S. DOI: http://dx.doi.org/10.1158/1078-0432.CCR-050004

[5] Goetz MP, Callstrom MR, Charboneau JW, et al. "Percutaneous image-guided radiofrequency ablation of painful metastases involving bone: a multicenter study". Journal of Clinical Oncology. January 2004. Vol. 22-2. p.300-306. DOI: http://dx.doi.org/10.1200/JCO.2004.03.097

[6] Martel J, Bueno A, Ortiz E. "Percutaneous radiofrequency treatment of osteoid osteoma using cool-tip electrodes". European Journal of Radiology. December 2005. Vol. 56-3. p.403-408. DOI: http://dx.doi.org/10.1016/j.ejrad.2005.05.014

[7] Lamuraglia M, Lassau N, Garbay JR, et al. "Doppler US with perfusion software and contrast medium injection in the early evaluation of radiofrequency in breast cancer recurrences: a prospective phase II study". European Journal of Radiology. December 2005. Vol. 56-3. p.376-381. DOI: http://dx.doi.org/10.1016/j.ejrad.2005.06.003

[8] Agnese DM, Burak WE Jr. "Ablative approaches to the minimally invasive treatment of breast cancer". Cancer Journal. February 2005. Vol. 11-1. p.77-82. DOI: http://dx.doi.org/10.1097/00130404-200501000-00012

[9] Huston TL, Simmons RM. "Ablative therapies for the treatment of malignant diseases of the breast". American Journal of Surgery. June 2005. Vol. 189-6. p.694-701. DOI: http://dx.doi.org/10.1016/j.amjsurg.2005.03.011

[10] Bojarski JD, Dupuy DE, Mayo-Smith WW. "CT imaging findings of pulmonary neoplasms after treatment with radiofrequency ablation: results in 32 tumors". American Journal of Roentgenology. August 2005. Vol. 185-2. p.466-471. DOI: http://dx.doi.org/10.2214/ajr.185.2.01850466

[11] Fitzpatric JM. "The role of registration in accurate surgical guidance". Proceedings of the Institution of Mechanical Engineers, Part H: Journal of Engineering in Medicine. May 2010. Vol. 224-5. p.607-622. DOI: http://dx.doi.org/10.1243/09544119JEIM589

[12] dos Santos TR, Seitel A, Meinzer HP, et al. "Correspondences search for surface-based intra-operative registration". Lecture Notes in Computer Science. September 2010. Vol.6362. p.660-667. DOI: http://dx.doi.org/10.1007/978-3-642-15745-5_81

[13] Shamir RR, Freiman M, Joskowicz L, et al. "Surface-based facial scan registration in neuronavigation procedures: a clinical study". Journal of Neurosurgery. December 2009. Vol. 111-6. p.1201-1206. DOI: http://dx.doi.org/10.3171/2009.3.JNS081457

[14] Luebbers HT, Messmer P, Obwegeser JA, et al. "Comparison of different registration methods for surgical navigation in cranio-maxillofacial surgery". Journal of Cranio-Maxillofacial Surgery. March 2008. Vol. 36-2. p.109-116. DOI: http://dx.doi.org/10.1016/j.jcms.2007.09.002

[15] Hong J, Hashizume M. "An effective point-based registration tool for surgical navigation". Surgical Endoscopy. April 2010. Vol. 24-4. p.944-948. DOI: http://dx.doi.org/10.1007/s00464-009-0568-2

[16] Zhang W, Wang C, Yu H, et al. "Effect of fiducial configuration on target registration error in image-guided cranio-maxillofacial surgery". Journal of Cranio-Maxillo-Facial Surgery. September 2011. Vol. 39-6. p.407-411. DOI: http://dx.doi.org/10.1016/j.jcms.2010.10.008

[17] Wang M, Song Z. "Improving target registration accuracy in image-guided neurosurgery by optimizing the distribution of fiducial points". International Journal of Medical Robotics and Computer Assisted surgery. March 2009. Vol. 5-1. p.26-31. DOI: http://dx.doi.org/10.1002/rcs.227

[18] Shamir RR, Joskowicz L, Shoshan Y. "Fiducial optimization for minimal target registration error in image-guided neurosurgery". IEEE Transactions on Medical Imaging. March 2012. Vol. 31-3. p.725-737. DOI: http://dx.doi.org/10.1109/TMI.2011.2175939

[19] Wiles AD, Thompson DG, Frantz DD. "Accuracy assessment and interpretation for optical tracking systems". Proceedings of SPIE-The International Society for Optical Engineering. February 2004. Vol. 5367. p. 421-432. DOI: http://dx.doi.org/10.1117/12.536128

[20] Lorensen WE, Cline HE. "Marching cubes: A high resolution 3D surface construction algorithm". Computer Graphics. July 1987. Vol. 21-4. p.163-169. DOI: http://dx.doi.org/10.1145/37401.37422

[21] Zhang, J. "An efficient median filter based method for removing random-valued impulse noise". Digital Signal Processing. July 2010. Vol. 20-4. p.1010-1018. DOI: http://dx.doi.org/10.1016/j.dsp.2009.11.003

[22] Suzukia K, Horibaa I, Sugieb N. "Linear-time connected-component labeling based on sequential local operations". Computer Vision and Image Understanding. January 2003. Vol. 89-1. p.1-23. DOI: http://dx.doi.org/10.1016/S1077-3142(02)00030-9